

Branched-Selective Hydroformylation of Non-Activated Olefins Using a N-Triphos/Rh Catalyst

*Andreas Phanopoulos and Kyoko Nozaki**

Department of Chemistry and Biotechnology, Graduate School of Engineering, The University of Tokyo, 7-3-1 Hongo, Bunkyo-ku, Tokyo 113-8656, Japan

Abstract

We report a catalytic system comprised of nitrogen-centered di- or triphosphine ligands in conjunction with rhodium that is capable of delivering branched aldehydes from terminal olefin substrates which commonly give more linear aldehydes than branched. The incorporation of an apical nitrogen atom into the ligand backbone dramatically improves the reaction rate. Mechanistic and labelling studies suggest the unusual selectivity is due to the irreversible trapping of the Rh–alkyl species along the branched pathway, in comparison to the more reversible linear pathway. A pre-catalytic equilibrium mixture of rhodium species was observed by high-pressure *in situ* NMR spectroscopy, suggesting this equilibrium is the catalytic resting state.

Key words: N-Triphos, rhodium, branched-selective, non-activated olefin, irreversible branched pathway

Introduction

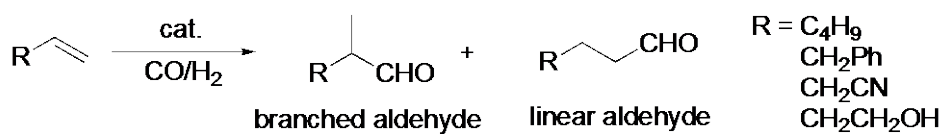
The production of aldehydes from olefins *via* hydroformylation annually amounts to a global production of more than 10 million tons of so-called “oxo” products.^[1] As such, it is one of the most extensively studied homogeneous catalytic processes in both academia and industry.^[2] Due to the commercial interest in plasticizers derived from linear alcohols (*e.g.* *bis*(2-ethylhexyl)phthalate derived from *n*-butanal),^[1a] the production of linear aldehydes have traditionally been the most desired products, with many known catalysts now capable of very high linear-selectivity.^[3]

Branched aldehydes, which result from the branched-selective hydroformylation of terminal olefins, usually require special substrates, such as allenes, vinylarenes or vinylacetate to ensure high regioselectivity.^[1,4,5] In this context, the branched-selective transformation of easily available bulk terminal olefins represents a challenging but increasingly desirable reaction. These products would have broad utility in the fragrance and flavor, and life-sciences industries, as well as being important intermediates in organic synthesis.^[6]

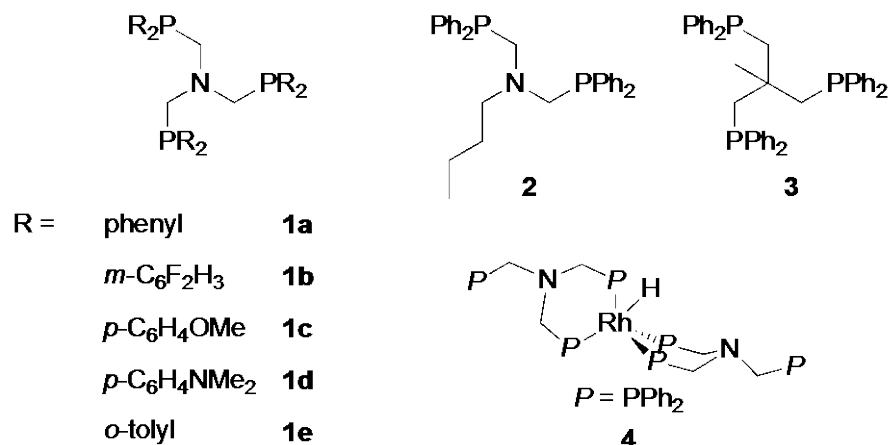
To date, few examples of catalyst systems capable of performing branched-selective hydroformylation of non-activated terminal olefins have been reported.^[7] Two notable examples of highly selective systems that represents the current state-of-the-art for this reaction are a rhodium encapsulation complex reported by Reek and co-workers^[8] and a Rh/BOBPHOS system reported by Clarke and co-workers.^[9,10] The former is constructed from a tripyridylphosphine ligand that coordinates to a rhodium center through phosphorus, and three metallo–porphyrin

units via the three nitrogens within the pyridyl moieties of the ligand (Chart 1, bottom left). Reek's encapsulated rhodium catalyst is able to distinguish between not only the 1- and 2-positions of 1-octene, but also between the 2- and 3-positions of *trans*-oct-2-ene.^[8f] Similar internal olefin differentiation has also been reported using a bulky *tris*-binaphthyl monophosphite ligand, but in this case the selectivity was proposed to stem from favorable interactions between the metal center and terminal ester groups incorporated within the substrate.^[11]

The Clarke system utilizes a phosphite–phospholane bidentate ligand (Chart 1, bottom right), and owes its branched-selectivity to subtle substrate–ligand interactions that render otherwise low energy pathways to linear aldehydes unproductive.^[10] This system shows not only high branched selectivity for a range of substrates including alkyl olefins and allyl arenes, but also delivers chiral aldehydes with a high degree of enantiomeric selectivity.^[9a] Beyond an academic setting, the Rh/BOBPPOS system has been used for the hydroformylation of allylglycine derivatives, capable of affording a chiral intermediate that is a key compound for the synthesis of new antibiotics.^[9b]



Ligands and complexes discussed in this work



cf. Ligands previously reported for branch-selective Rh-catalyzed hydroformylation

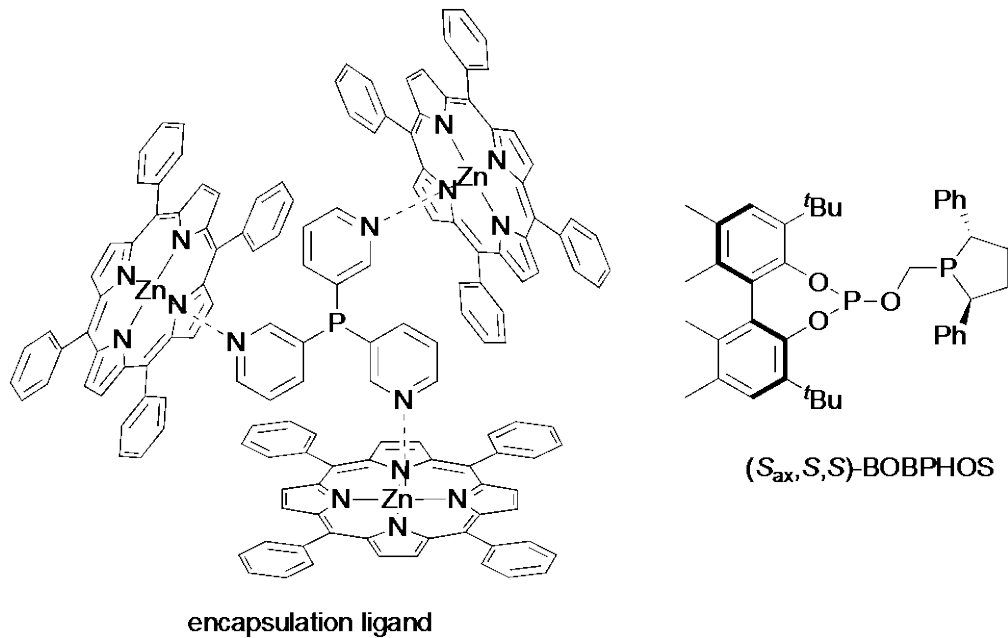
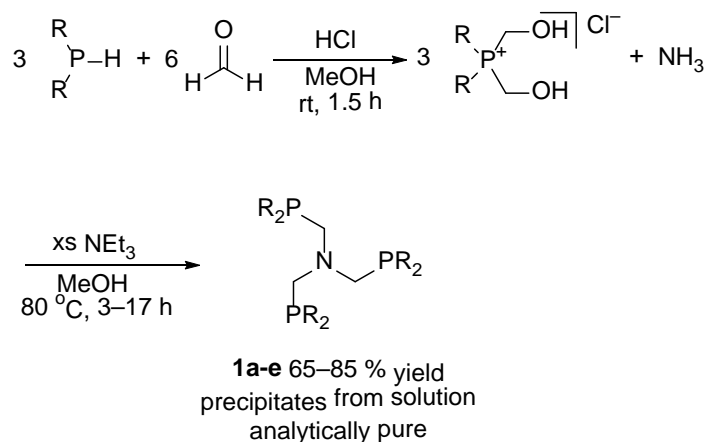


Chart 1. Branched-selective Rh-catalyzed hydroformylation of olefins. The ligands and complex discussed in this study (center) and ligands reported in previous studies (bottom).

Herein, we report a simple achiral catalyst system formed *in situ* from nitrogen-centered di- or triphosphine ligands **1** and [Rh(acac)(CO)₂] (acac = acetylacetonate) and their application to the hydroformylation of terminal olefins described in Chart 1, top. While the substrates commonly undergo linear-selective hydroformylation, rather unusual branched-selectivities were detected in this study. The triphosphine ligand **1a** remained selective even at relatively low loadings and temperatures, while bidentate ligand **2** afforded predominantly linear aldehydes under these conditions. The results will be discussed in comparison to the conventional triphosphine ligand **3**. Isolation of *bis*-ligated complex **4** and its behavior as a catalyst precursor are also discussed.

Results and Discussion

1. Hydroformylation of 1-hexene catalyzed by Rh complexes of aza-triphosphine ligands 1a–e. The tridentate ligands **1a–e** were synthesized in a modular fashion by adapted literature procedures,^[12] allowing facile generation of a series of tridentate phosphine ligands with various substituents on the phosphorus atom (Scheme 1). With this family of ligands in hand, we investigated their competency for the hydroformylation of 1-hexene as a model substrate when combined with [Rh(acac)(CO)₂] *in situ*. In addition, we compared the nitrogen-centered ligands (**1a–e** and **2**) with the carbon-centered analogue, CH₃C(CH₂PPh₂)₃ (**3**).



Scheme 1. Synthetic procedure for the facile generation of ligands **1a–e**.

1.1. Catalytic Study with $[\text{Rh}(\text{acac})(\text{CO})_2]/\mathbf{1a}$.

As a starting point, *tris*(diphenylphosphinomethyl)amine **1a** was used in conjunction with $[\text{Rh}(\text{acac})(\text{CO})_2]$ as the catalyst for the hydroformylation of 1-hexene. Representative results are summarized in Table 1. In all cases, only 1-heptanal and 2-methylhexanal products were observed unless otherwise stated. When the reaction was performed with 1 mol % Rh loading, a Rh:L = 1:2 at 100 °C under CO/H₂ (1:1) = 2.0 MPa for 3.5 h ([Rh] = 5 mM, [L] = 10 mM), this resulted in the production of aldehydes in high yields and a slight regioselective bias towards the branched product (99.4%, *b/l* = 1.10, Table 1, entry 1). This was somewhat unexpected, as the structurally related carbon-centered ligand *tris*(diphenylphosphinomethyl)ethane (**3**) was reported to be linear-selective under only slightly different conditions (*b/l* = 0.22–0.93).^[13,14] To establish whether the divergent regioselectivities are a direct result of the introduction of an apical nitrogen atom to the ligand, a control experiment using **3** under identical conditions was conducted (Table 1, entry 2). In this case, unlike the reported data, slightly improved branched-selectivity was observed but at the expense of a greatly reduced rate, thus only 16.1% of 1-hexene was consumed (see 2.4. *Proposal for the active species and catalytic cycle* for further

discussion). In the presence of ligand, no isomerization of 1-hexene to 2-hexene or 3-hexene was observed, however a control reaction without ligand afforded aldehydes derived from isomerized hexenes as well as hydrogenated side-product hexane (Table 1, entry 3). The bite angle of multidentate ligands has previously been shown to influence the regioselectivity during hydroformylation. The bite angle for **1a** when coordinated to Rh^I cannot be assessed with great precision due to the absence of published crystal structures, but low-quality data obtained within our laboratory has allowed us to estimate its bite angle to be 88°, while that of carbon-centered **3** is 89° based on crystal structure data. Consequently, bite angle does not appear to be a differentiator between these two ligands.

Table 1. Hydroformylation of 1-hexene with azatriphos (**1a**)/Rh under various reaction conditions^a

Entry	Temp. (°C)	[Rh] (mM)	<i>p</i> CO (MPa)	<i>p</i> H ₂ (MPa)	CHO (%) ^b	TOF (h ⁻¹)	<i>b/l</i> ^b	Comment
1 ^c	100	5.0	1.0	1.0	99.4	28	1.10	Standard
2 ^d	100	5.0	1.0	1.0	16.1	4.6	1.27	Control with 3
3 ^{c,e}	100	5.0	1.0	1.0	85.6	24	1.11	Control without ligand
4	100	5.0	1.0	1.0	71.4	71	1.06	Temperature (Figure 1)
5	90	5.0	1.0	1.0	33.9	34	1.12	
6	80	5.0	1.0	1.0	15.9	16	1.22	
7	70	5.0	1.0	1.0	6.30	6.3	1.41	
8	60	5.0	1.0	1.0	2.80	2.8	1.92	
9	50	5.0	1.0	1.0	0.84	0.8	5.46	
10 ^c	25	5.0	1.0	1.0	0.00	0.0	---	

11 ^c	100	2.5	1.0	1.0	90.3	181	1.09	
12 ^c	100	1.25	1.0	1.0	72.4	290	1.05	[Rh]
13 ^c	100	0.25	1.0	1.0	24.4	488	1.10	
14	100	5.0	0.5	1.0	83.9	84	1.09	
15	100	5.0	1.5	1.0	53.8	54	1.11	<i>p</i> CO
16	100	5.0	3.0	1.0	27.7	28	1.13	(Figure S56)
17	100	5.0	1.0	0.5	56.3	56	1.08	
18	100	5.0	1.0	1.5	70.6	71	1.07	<i>p</i> H ₂
19	100	5.0	1.0	3.0	75.0	75	1.07	(Figure S58)

^aReaction conditions: toluene (3.75 mL), 1-hexene (250 μ L, 500 mM), [Rh] = [Rh(acac)(CO)₂],

L = **1a**, Rh:L = 1:2, 1 h; branched and linear aldehydes were the only products in all cases.

^bDetermined by GC, confirmed by NMR; *b* = 2-methylhexanal, *l* = 1-heptanal. ^c3.5 h. ^d3.5 h, L =

3. ^eNo ligand, hexane formed (12.4%).

In order to investigate the reaction mechanism several parameters were examined, including temperature, substrate and catalyst concentration, and partial pressures of CO and H₂. Firstly, temperature was varied from 25–100 °C at constant CO/H₂ pressure (Table 1, entries 4–10). At lower temperatures a significant increase in selectivity is observed (*b/l* up to 5.46 at 50 °C); but at temperatures below 100 °C the overall activity is also significantly reduced (Figure 1), with no reaction occurring at room temperature over 3.5 hours under 2.0 MPa CO/H₂ (Table 1, entry 10). Reducing the catalyst loading from 1.0–0.05 mol % ([Rh] = 5–0.025 mM) while keeping the Rh:L ratio at 1:2 ([L] = 10–0.05 mM) did not affect the selectivity (Table 1, entries 11–13). This suggests higher nuclearity species, for instance dimeric compounds with Rh–Rh bonds or featuring **1a** in a bridging mode between two Rh centers, are less likely to be responsible for the

observed selectivity (*vide infra*). Additionally, kinetic analysis of the rate compared to [Rh] and [1-hexene] revealed both to be first order (Figure S54 and S55), suggesting coordination of olefin to a monometallic active species to be rate-determining.

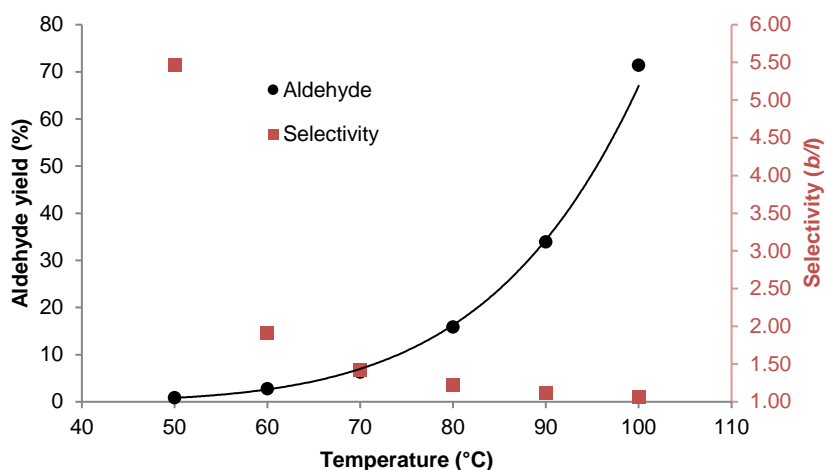


Figure 1. Temperature dependence of total yield of aldehydes and *b/l* selectivity for data in entries 4–9 in Table 1.

Varying the partial pressure of CO had a dramatic effect on catalyst activity, with increased pressures severely hindering the reaction (Table 1, entries 14–16). In parallel to decreasing the overall reaction rate, a small increase in regioselectivity towards the branched product was observed, with *b/l* increasing from 1.09 to 1.13 when CO pressure is increased from 0.5 to 3.0 MPa at 100 °C. To probe the dependence on CO pressure further, this parameter was also evaluated at 50 °C, as this temperature was shown to promote the formation of branched products (Figure S57). Again, a similar decrease in catalyst activity was observed with increasing CO pressure, while overall the selectivity also increased from 1.60 to 2.09 as the CO pressure is increased from 0.2 to 2.0 MPa. A slightly lower pressure range was used for the

analysis at 50 °C as at pressures above 2.0 MPa at this temperature only trace amounts of products are formed, making accurate analysis impossible. In fact, even at 2.0 MPa, very small amounts of aldehydes were formed (<2%), with values approaching the accurate detection limits of the instruments. Consequently, although a general increase in branched selectivity was observed with CO pressure, this relationship needs to be evaluated to a greater degree of accuracy for conclusive results. Other mechanistic studies have also shown that CO pressure can significantly affect the regioselectivity observed during hydroformylation, normally to a much greater degree.^[15] For instance, Rosales *et al.* reported that during the hydroformylation of 1-hexene with ligand **3**, increasing the CO pressure from 0.1 to 0.55 MPa resulted in an increase in *linear* aldehydes from $l/b = 1.5$ to 5.8.^[14] Under their catalytic conditions, olefin coordination is regio-determining, and is consequently highly affected by CO pressure which competes for coordination to the metal center. On the other hand, the regio-determining step in the present system is likely to be hydride migration (see section 2.1. *Deuterioformylation*) and is consequently less effected by CO pressure. The partial pressure of H₂ had a smaller effect on the activity, showing only a slight rate enhancement at high pressures, and also had no effect on the selectivity (Table 1, entries 17–19). Preliminary kinetic analysis of this data at 100 °C shows an order of -0.6 in p_{CO} and +0.15 in p_{H_2} (Figures S54 and S56, respectively).

1.2. Comparison of ligands **1a–1e**: Electronic and steric effects

By modulating the substituents at phosphorus, the electronic and steric properties of the ligand can be easily tuned. To this end, several triphosphine derivatives were examined that contain various groups at phosphorus (Table 2). The introduction of electron withdrawing *meta*-difluorophenyl substituents (**1b**)^[12c] did not retard the rate, but did alter the selectivity towards

more linear-selective products (Table 2, entry 1). On the other hand, the incorporation of electron-donating but sterically small substituents *para*-methoxyphenyl (**1c**) or *para*-*N,N*-dimethylaminophenyl (**1d**) improves the branched-selectivity marginally (Table 2, entries 2 and 3) with a concomitant decrease in activity. This implies there is a slight electronic preference for branched aldehyde formation with increasingly electron-donating ligands.

The electronic nature of coordinating ligands has been extensively explored for mono- and bidentate systems during hydroformylation. In general, less basic phosphorus containing moieties such as (di)phosphites (rather than phosphines) afford aldehydes with greater linear selectivity.^[16,17] This was reasoned to be due to faster β -hydride elimination from the branched Rh-alkyl species but not the linear species.^[16a] In the present system, however, formation of the branched Rh-alkyl complex is suggested to be irreversible (see section 2.1. *Deuterioformylation*), so the observed effect must be more subtle. In a separate line of thought, the regioselectivity dependence on ligand electronic parameters was thought to originate from a perturbation of the equatorial-equatorial:equatorial-axial (ee:ea) isomer ratio present during catalytic turnover when bidentate ligands are used. Upon changing the electron donating ability across a series of diphosphine ligands, the resultant complexes showed a higher proportion of the ee isomer, which is known to give more linear aldehydes.^[18–20] Subsequent investigations, however, have revealed this relationship to be primarily steric in nature.^[17,20] In the present system, the more basic ligand could have caused the higher ‘hydricity’ of the Rh-H species^[21] to increase the proportion of branched Rh-alkyl species present since the terminal olefinic carbon is more positive than the internal one.^[22] As for the reaction rate, electron donating ligands generally lower the hydroformylation rate due to a strengthening of the Rh-CO bonds, retarding CO dissociation and the formation of the required unsaturated species for olefin coordination.^[17]

As may be expected, the use of an electron-donating but sterically encumbering substituent, *ortho*-tolyl (**1e**), results in an increased linear bias (Table 2, entry 6), presumably due to localized steric pressure around the metal center.

As had been confirmed by the temperature dependence study, lowering the temperature from 100 to 50 °C gave improved branched-selectivity using **1a** as the ligand. Indeed, under otherwise standard conditions (*i.e.* 3.5 h, CO/H₂ (1:1) = 2.0 MPa, [Rh] = 5 mM, [L] = 10 mM), reducing the temperature to 50 °C, increased *b/l* from 1.10 at 100 °C to 1.66 using **1a** (Table 1, entry 1 and Table 2, entry 7). A similar selectivity enhancement was observed for the most branched-selective ligand, **1d** (Table 2 entries 3 and 4), showing very high selectivity at 50 °C (*b/l* = 5.91), albeit with low activity.

To increase the activity and maintain high branched-selectivity, low CO pressures (0.2 MPa) and low temperatures (50 °C) were implemented using **1a** and **1d** as ligands. Utilizing **1a**, conversion was relatively high, while selectivity was somewhat reduced compared to the standard conditions (Table 2, entry 8). This further suggests higher CO pressures are indeed beneficial for the formation of branched aldehydes. Still, this represents one of the best catalytic systems capable of producing large quantities (>80% conversion) of branched aldehydes (*b/l* = 1.29) using relatively short reaction times (24 hours) reported to date. For comparison, the BOBPHOS system gave 78% conversion after 46 hours (*b/l* = 3.0) for 1-hexene, and additionally showed high selectivity and activity across a series of unactivated olefins (*b/l* > 4 and TOF up to 417 h⁻¹).^[9a] Using **1d** under these low pressure and temperature conditions resulted in significant amounts of hydrogenated products (68% hexane), and showed poor selectivity (Table 2, entry 5). In this case, the migration of CO to form a Rh–acyl is likely severely retarded due to the low CO

pressure, and strong Rh–CO bond from the increased electron density at rhodium from the donating ligand.

Table 2. Catalytic data for the hydroformylation of 1-hexene with different azatriphos ligands^a

Entry	Catalyst	Temp. (°C)	<i>p</i> CO (MPa)	<i>p</i> H ₂ (MPa)	CHO (%) ^b	TOF (h ⁻¹)	<i>b/l</i> ^b
1 ^c	[Rh]/ 1b	100	1.0	1.0	97.7	28	0.92
2 ^c	[Rh]/ 1c	100	1.0	1.0	79.2	23	1.11
3 ^c		100	1.0	1.0	57.8	17	1.16
4 ^c	[Rh]/ 1d	50	1.0	1.0	0.76	0.2	5.91
5 ^{d,e}		50	0.2	0.8	6.21	0.3	0.99
6	[Rh]/ 1e	100	1.0	1.0	70.9	20	0.43
7 ^c	[Rh]/ 1a	50	1.0	1.0	4.81	1.4	1.66
8 ^e		50	0.2	0.8	82.9	3.5	1.29
9	4	100	1.0	1.0	89.4	26	1.10
10		50	1.0	1.0	6.33	1.8	1.48

^aReaction conditions: toluene (3.75 mL), 1-hexene (250 μL, 500 mM), [Rh] = [Rh(acac)(CO)₂]

(1.0 mol %, 5 mM), **1** (2.0 mol %, 10 mM), CO (1.0 MPa), H₂ (1.0 MPa), 3.5 h; branched and linear aldehydes were the only products in all cases unless otherwise stated. ^bDetermined by GC, confirmed by NMR; *b* = 2-methylhexanal, *l* = 1-heptanal. ^cAverage of two separate runs.

^dSignificant hexane formed (67.9%). ^e24 h.

1.3. Comparison with aza-diphosphine ligand **2**.

Mechanistic studies suggest that during catalysis the triphosphine ligands only coordinates to rhodium through two arms, leaving one free phosphine ‘dangling’ (*vide infra*). This begs the question as to whether the third arm of each ligand is necessary for the observed regioselectivity.

To this end, a diphosphine ligand, *n*BuN(CH₂PPh₂)₂ (**2**) that contains a *n*-butyl carbon chain instead of a third phosphine arm,^[23] was evaluated and showed similar catalytic activity to **1a** under standard reaction conditions ([Rh] = 5 mM, [L] = 10 mM, 100 °C, CO/H₂ (1:1) = 2.0 MPa: Table 3, entries 1 and 5). However, at lower ligand loadings ([L] = 5 mM) under optimized CO/H₂ pressures (0.2/0.8 MPa) and low temperatures (25–50 °C), the tridentate **1a** system not only maintains, but shows greater branched-selectivity (Table 3, entry 4), while the bidentate **2** system changes to give predominantly linear aldehydes (Table 3, entry 8). Additionally, at lower ligand loadings using **2** afforded more hexane (2%) in contrast to **1a**, which remains highly chemoselective.

These observations show that under these conditions there is a switch in regioselectivity depending on whether di- or triphosphine ligands are used. This may be due to a change in regio-determining step, or the result in different speciation at lower temperatures. Although we are uncertain what change is responsible, it is clear that the tridentate ligand engenders divergent reactivity compared to the bidentate analogue.

Table 3. Catalytic data for the hydroformylation of 1-hexene comparing bi- and tridentate ligands^a

Entry	Catalyst	[Rh] (mM)	[L] (mM)	Temp. (°C)	<i>p</i> CO (MPa)	<i>p</i> H ₂ (MPa)	CHO (%) ^b	TOF (h ⁻¹)	<i>b/l</i> ^b
1	[Rh]/ 1a	5.0	10	100	1.0	1.0	99.4	28	1.10
2		5.0	5.0	100	1.0	1.0	90.1	26	0.99
3 ^c		5.0	5.0	50	0.2	0.8	66.3	2.8	1.30
4 ^c		5.0	5.0	25	0.2	0.8	3.73	0.2	2.06
5	[Rh]/ 2	5.0	10	100	1.0	1.0	93.1	27	1.10

6	5.0	5.0	100	1.0	1.0	>99.9	29	1.07
7 ^c	5.0	5.0	50	0.2	0.8	99.4	4.1	1.26
8 ^c	5.0	5.0	25	0.2	0.8	35.4	1.5	0.54

^aReaction conditions: toluene (3.75 mL), 1-hexene (250 μ L, 500 mM), [Rh] = [Rh(acac)(CO)₂]

(1.0 mol %), 3.5 h; branched and linear aldehydes were the only products in all cases unless otherwise stated. ^bDetermined by GC, confirmed by NMR; *b* = 2-methylhexanal, *l* = 1-heptanal.

^c24 h.

1.4. Substrate scope.

Next the substrate scope for this catalytic system was evaluated with several terminal olefins which have previously been targeted for branched-selective hydroformylation (Table 4).^[9a,10,24] These substrates were subjected to the standard hydroformylation conditions using both **1a** and **2** as ligands. Substrates with phenyl (Table 4, entries 1 and 4) and cyano groups were investigated (Table 4, entries 2 and 5), as well as an alcoholic substrate, 3-butenol (Table 4, entries 3 and 6).

Allylbenzene was found to perform similar to 1-hexene, producing only aldehydes and predominantly branched-selective products (*b/l* = 1.33) whether ligand **1a** or **2** were used. Allyl cyanide showed exceptionally high branched-selectivity (up to *b/l* = 6.12), with **1a** performing better than **2**, but with greatly reduced chemoselectivity compared to substrates without heteroatoms (31.8–40.2% selectivity for aldehyde products). 3-Butanol, on the other hand, did not afford aldehyde products at the end of the reaction, as both linear and branched products had been cyclized to form lactols (Scheme 2). The amount of five- versus six-membered ring lactols allows us to determine how much branched and linear aldehydes had been formed, respectively,

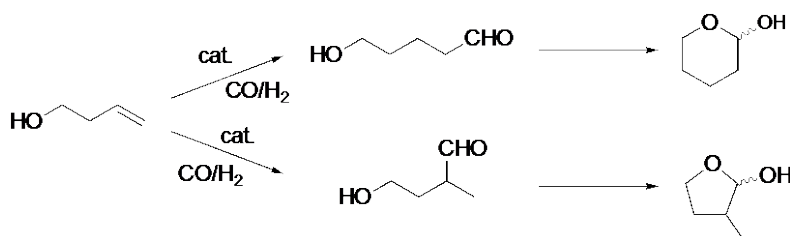
giving a selectivity of $b/l = 1.33$ – 1.39 depending on which ligand was used. Again, despite giving lactol products, the alcoholic moiety did not affect the regioselectivity of the system.

Table 4. Catalytic data for the hydroformylation of various substrates using ligands **1a** and **2a**

Entry	Catalyst	Substrate	Aldehydes/Cyclised Products		
			Yield (%) ^b	TOF (h ⁻¹)	b/l^b
1	[Rh]/ 1a	allylbenzene	99.8	29	1.33
2		allyl cyanide	40.2	11	6.12
3		3-butenol	99.2	28	1.39 ^c
4	[Rh]/ 2	allylbenzene	99.7	29	1.32
5		allyl cyanide	31.8	9.1	4.98
6		3-butenol	97.4	28	1.33 ^c

^aReaction conditions: toluene (total volume 4.0 mL), substrate (2 mmol, 500 mM), [Rh] = [Rh(acac)(CO)₂] (1.0 mol %, 5 mM), ligand (2.0 mol %, 10 mM), 100 °C, CO/H₂ (1:1) = 2.0 MPa, 3.5 h. ^bDetermined by NMR, in each case starting material showed quantitative conversion.

^cFive-membered lactol/six-membered lactol.



Scheme 2. Hydroformylation of 3-butenol and subsequent cyclization to form lactols.

2. Mechanistic studies. Recently, Clarke and co-workers reported a similar kinetic profile for the asymmetric hydroformylation of allylbenzene using BOBPHOS as that observed in the current system, both of which showed high branched-selectivity.^[10] Additionally, several kinetic studies of diphosphine systems have also been reported, which revealed similar CO and H₂ dependencies.^[25] Several energetically similar steps were found to contribute to the overall rate of the reaction, including the olefin insertion/hydride transfer and product forming hydrogenolysis steps, suggesting a similar mechanism may be operational in this work. In Clarke's BOBPHOS system, the selectivity was determined during an irreversible olefin insertion step to Rh–H, which was confirmed by a labeling study. In the present study with Rh/**1a**, the olefin insertion step is also likely to be regio-determining as neither substrate concentration nor H₂ pressure affected the *b/l* ratio (Table 1, entries 17–19). To confirm whether the olefin insertion is reversible or not, a deuterioformylation study was first conducted.

2.1. Deuterioformylation

By treatment of 1-hexene with D₂ and CO in the presence of Rh/**1a**, it was confirmed that hydride migration is largely irreversible for branched Rh–alkyl formation, while it is reversible for linear Rh–alkyl formation. The deuterioformylation was conducted using [Rh(acac)(CO)₂] (5 mM) and **1a** (10 mM) under a 1:1 CO/D₂ mixture at 1.0 MPa for 1 hour. The products were analyzed by ¹H, ²H and GC/GC-MS (Figure S59) and compared to previously reported deuterium incorporated products from the deuterioformylation of the same substrate.^[26] The results are summarized in Figure 2. The recovery of the unreacted 1-hexene was 20.4%. The branched aldehyde (branched-CHO) and the linear aldehyde (linear-CHO) with deuterium incorporated at the β-position to the -CDO group were obtained in 29.8% and 36.4% yield,

respectively. The other detected products were, 2-deuterio-1-hexene (hexene-2d, 5.6%) and branched product 2-methylhexanal with deuterium labels at the α - and aldehyde carbons (branched-CHO*, 2.7%), both of which are exclusive products from the reverse hydride migration from an initial linear Rh–alkyl intermediate. Notably, no products were observed that are the result of β -hydride elimination of a branched Rh–alkyl species such as hexene-1d or linear-CHO*. This demonstrates that formation of linear Rh–alkyl intermediates is somewhat reversible while formation of the analogous branched Rh–alkyl intermediate is not.

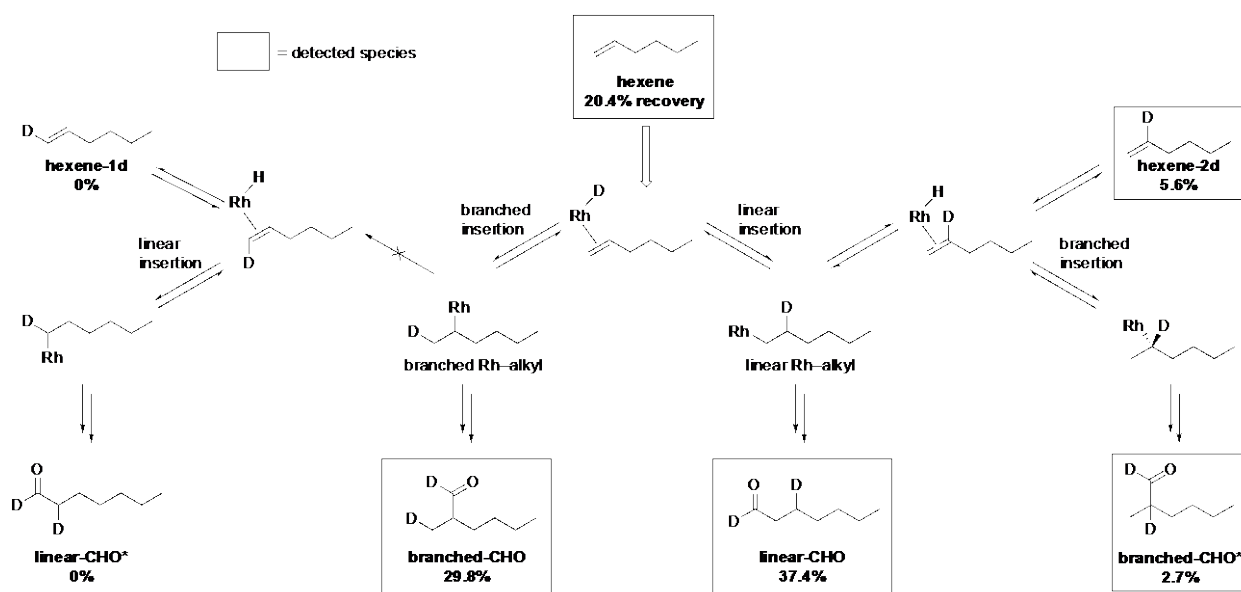
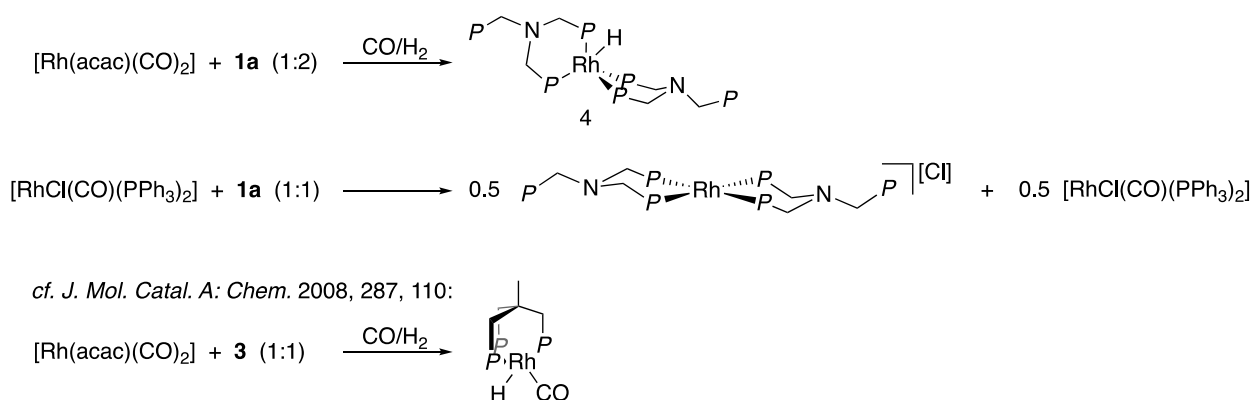


Figure 2. Graphical representation of the product distribution observed during deuterioformylation. Percentages represent total amounts based on initial substrate loading.

2.2. NMR studies in the absence of olefin.

The following NMR studies provided some information towards determining the identity of potentially active species. After subjecting the pre-catalytic 1:2 mixture of $[\text{Rh}(\text{acac})(\text{CO})_2]$ and azatriphos **1a** to the catalytic conditions ($[\text{Rh}] = 5 \text{ mM}$, $[\mathbf{1a}] = 10 \text{ mM}$, CO/H_2 (1:1) = 2.0 MPa,

100 °C, 0.5 h), the major species detected after removal of the solvent and any volatiles was the *bis*-ligated monohydride complex $[\text{RhH}(\kappa^2\text{-}\mathbf{1a})_2]$ (**4**) by $^{31}\text{P}\{^1\text{H}\}$ NMR (δ_{P} : 15.4 (d, $^1J_{\text{PRh}} = 141.0$ Hz, 4P), -30.9 (s, 2P)) (Scheme 3). This was confirmed to be the correct assignment by a separate synthesis (see Supporting Information), and in solution is probably tetrahedral with the hydride jumping from face to face, as evidenced from broadening of the hydride signal by ^1H NMR spectroscopy (Figure S46) as well as broadening of the coordinated phosphorus signals by $^{31}\text{P}\{^1\text{H}\}$ NMR spectroscopy at -50 °C (Figure S49).^[27] When complex **4** was used as the catalyst under otherwise identical conditions (Table 2, entries 9 and 10), the same reactivity and selectivity was observed as the *in situ* generated catalyst, confirming that this complex is at least a competent pre-catalytic species. Interestingly, this differs significantly from the carbon-centered triphos ligand **3**, with which the mono-ligated tridentate complex $[\text{RhH}(\text{CO})(\kappa^3\text{-}\mathbf{3})]$ was isolated and reported to be the catalytic resting state.^[14] Although the corresponding tridentate complex $[\text{RhH}(\text{CO})(\kappa^3\text{-}\mathbf{1a})]$ (**A**) with ligand **1a** was observed under pressures of CO/H₂ (*vide infra*), this complex is probably less stable compared to **4** (see section 2.5. *Comparison of azatriphos 1a and carbon-centered triphos 3* for further discussion). The propensity for *bis*- κ^2 -ligation of **1a** to Rh over κ^3 -ligation is evident from the reaction of **1a** with $[\text{RhCl}(\text{CO})(\text{PPh}_3)_2]$ in a 1:1 stoichiometry, which exclusively forms 0.5 equiv. $[\text{Rh}(\kappa^2\text{-}\mathbf{1a})_2][\text{Cl}]$ and leaves 0.5 equiv. $[\text{RhCl}(\text{CO})(\text{PPh}_3)_2]$ unreacted (Scheme 3).



Scheme 3. Formation of *bis*-ligated complex **4** with **1a** and mono-ligated complex with **3**.

The catalyst precursor **4** was converted to Rh carbonyl complexes upon treatment with CO or with a mixture of CO and H₂ as shown in Figure 3. Exposure of complex **4** (7.5 mM) in C₆D₆ to CO (5 bar) provided an equilibrium mixture of several species (Figure 3, top). The three major species in equilibrium have been assigned as [RhH(CO)(κ³-**1a**)] (**A**), [Rh(CO)(μ-CO)(κ²-**1a**)₂] (**B**), and [RhH(CO)₂(κ²-**1a**)] (**C**) based on ¹H, ¹³C{¹H} ³¹P{¹H}, ¹H-³¹P HMBC and DOSY NMR spectroscopy (Figures S58–S63), as well as by comparison to similar reported compounds (see Supporting Information for discussion on assignment).^[14,28] These three species existed in the ratio **A**:**B**:**C** = 1.0:9.0:6.4 at room temperature and free **1a** and H₂ (from the formation of dimeric **B**, 76% accounted for by ¹H NMR spectroscopy) were also observed. Two species (**B** and **C**) were observed when **4** was treated with CO/H₂ (1:1, 5 bar), in a ratio of **B**:**C** = 1.0:2.4 at 25 °C (Figure 3, bottom). The considerably broader peaks detected by ¹H NMR spectroscopy suggest increased fluxionality in comparison to exposure to only CO. Heating the mixture of **4**/CO/H₂ from 25–80 °C resulted in the formation of species **A** in addition to **B** and **C**, while cooling back to 25 °C reestablishes the original equilibrium mixture (Figure S66). When these experiments were performed using a 1:2 mixture of [Rh(acac)(CO)₂] and **1a** instead of pre-formed **4**, the same equilibrium mixture of **A**–**C** was observed.

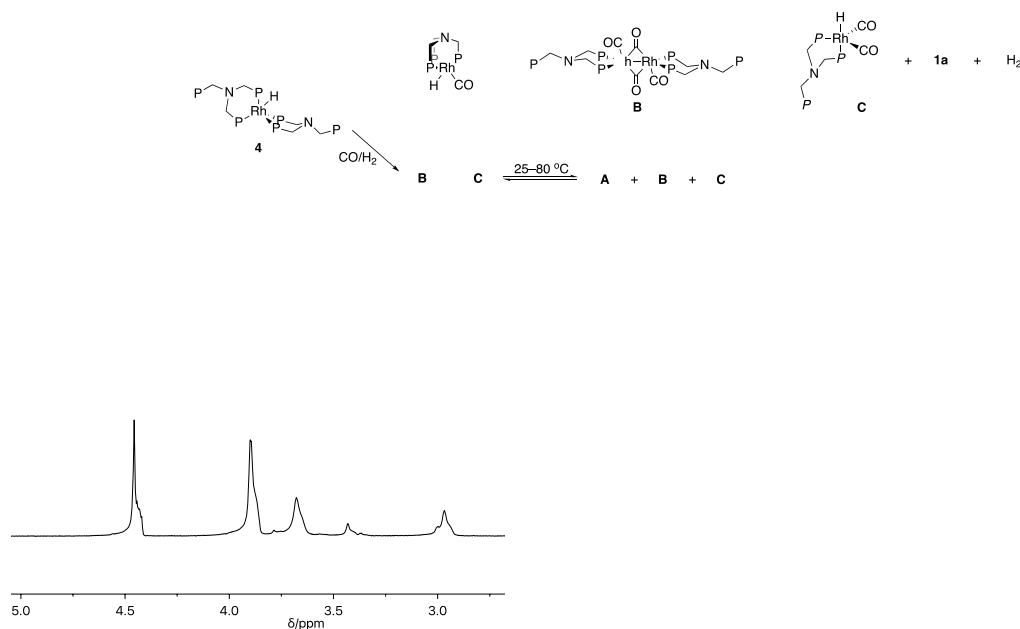


Figure 3. Stacked ¹H NMR spectra of complex **4** under 5 bar CO (left top) and CO/H₂ (left bottom); stacked ¹H NMR spectra of hydride region of complex **4** under 5 bar CO (middle top) and CO/H₂ (middle bottom); and stacked ³¹P{¹H} spectra of complex **4** under 5 bar CO (right top) and CO/H₂ (right bottom): showing equilibrium mixture of species **A–C**.

2.3. NMR studies in the presence of olefin.

In an attempt to observe Rh–acyl species, the behavior of complex **4** in the presence of 1-hexene and either CO or CO/H₂ was investigated (Figure 4). In the absence of CO or H₂, complex **4** is unreactive towards 20 equiv. 1-hexene (Figure 4b). Although, Rh–acyl species could not be detected when the mixture of **4** and 1-hexene were exposed to CO (5 bar), an almost identical equilibrium mixture of species was observed as in the absence of olefin (**A**:**B**:**C** = 1.0:8.0:6.2, Figure 4c). Upon changing the atmosphere to H₂, aldehyde production was observed (Figure 4d);

suggesting at least one of the species generated from **4**/CO is active. Furthermore, a branched-selective bias in aldehyde production was observed ($b/l = 1.05$), supporting the involvement of these species within the actual catalytic cycle. On the onset of aldehyde production, the $^{31}\text{P}\{^1\text{H}\}$ NMR spectra are simplified, showing only two detectable species: **4** and **A** (Figure 4e–g). Complexes **4** and **A** are also the only resolvable species by $^{31}\text{P}\{^1\text{H}\}$ NMR spectroscopy when a mixture of **4** (12.6 mM) and 1-hexene (20 equiv.) are directly exposed to CO/H₂ (5 bar), with concomitant production of aldehyde, even at 25 °C under these low CO pressures. This further implicates olefin coordination after CO dissociation to be at least partially rate determining.

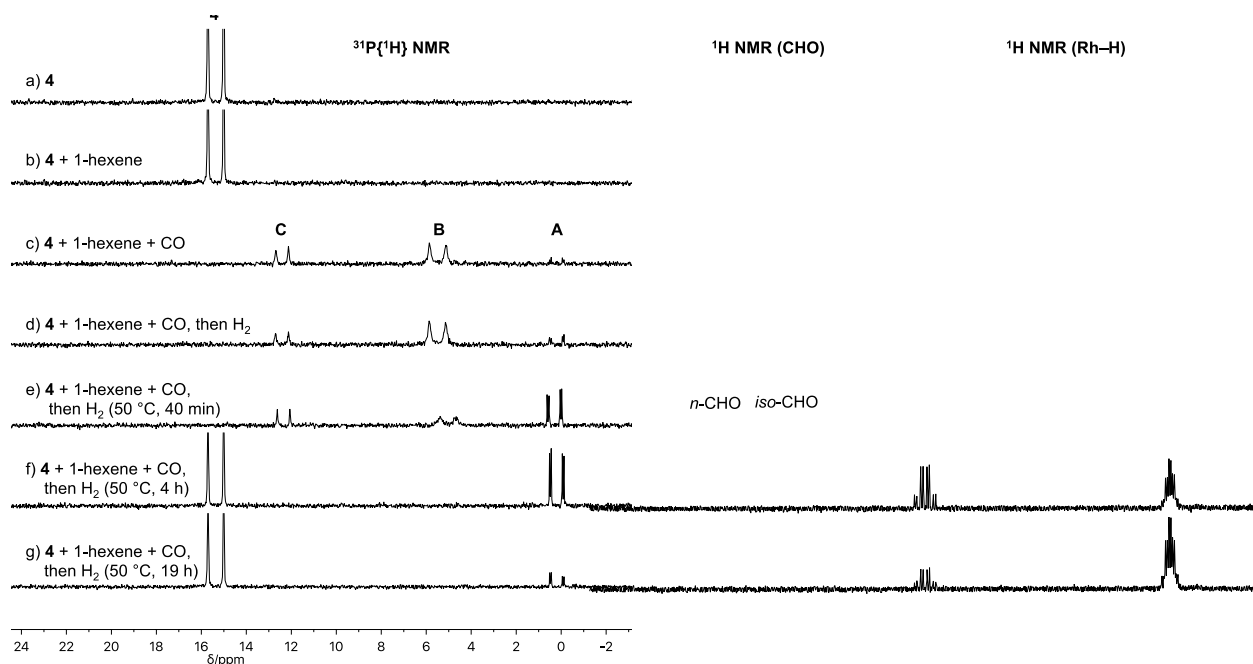


Figure 4. Stacked $^{31}\text{P}\{^1\text{H}\}$ NMR spectra showing sequential reaction of **4** with CO, then H₂ in the presence of 1-hexene (left) and stacked ^1H NMR spectra showing onset of aldehyde production (middle) and Rh–H signals (right).

2.4. Proposal for the active species and catalytic cycle.

Although only *bis*-ligated complex **4** and tridentate complex **A** are observed during catalytic turnover, these species must lie off-cycle as they are coordinatively saturated 18-electron compounds with no bound olefin, alkyl or acyl moiety. In order to account for the large negative dependence on CO pressure with respect to rate, the active catalytic species is likely to be present as a fast, unresolvable equilibrium on the NMR time-scale. From the mechanistic results, as well as the identification of **B** and **C**, the following catalytic cycle may be reasonably proposed (Figure 5). In this cycle, an equilibrium exists as the resting state, with only **4** and **A** in sufficient quantities or of sufficient lifetime to be detected by NMR spectroscopy during catalytic turnover. The dissociation of CO and subsequent olefin coordination to form olefin complex **E** is predominantly rate determining. Next, olefin insertion takes place accompanied by additional CO coordination to form linear or branched Rh–alkyl species **F**. While formation of the branched Rh–alkyl was irreversible, the formation of the linear Rh–alkyl species was proven to be reversible to some extent. In conjunction with higher CO pressures increasing branched selectivity, it seems the reversibility of the linear pathway acts to enhance an intrinsic propensity for branched Rh–alkyl formation during olefin insertion, making this step likely to be regio-determining. Once **F** is formed, CO insertion followed by hydrogenolysis of the Rh–acyl species completes the cycle.

Within the context of the present system, CO pressure was found to be the most important parameter in altering the rate of reaction, not H₂ pressure. Accordingly, formation of a species with a vacant site (species **D** in Figure 5) to allow olefin coordination is vital to improve the rate. With a bidentate coordinated **1a** or **3**, this vacant site could be occupied by olefin, CO or phosphine during catalysis.

In the case of **3**, we know the tridentate complex was the sole species observed under catalytic conditions,^[14] however ligand **1a** prefers to bind in a bidentate fashion (*e.g.* species **4**, **B** and **C**), therefore increasing the amount of unsaturated species present (Scheme 3 and Figure 3). We propose that the propensity of **1a** to *not* coordinate through all three phosphine groups due to electronic instability could be advantageous to form species **D** leading to the observed rate enhancement. The electronic instability when **1a** coordinates through all three phosphine moieties is due to the lone pair on the apical nitrogen, which is donated into the three flanking C^{methylene}-P σ*-orbitals, hindering backdonation from rhodium to phosphorus and resulting in a disproportionately electron rich metal center (Chart 2).^[12c,29] This electron donation does not exist for carbon-centered **3** which favors tridentate coordination due to chelation.^[14]

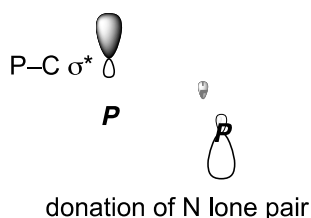


Chart 2. Electronic instability of tridentate coordination of **1a**.

Conclusions

In conclusion, a series of nitrogen-centered di- and triphosphine ligands have been synthesized with various substituents at phosphorus and tested in conjugation with Rh for the hydroformylation of terminal olefins. For 1-hexene, allylbenzene, allyl cyanide, and 3-butenol, branched-selectivity was observed, ultimately delivering branched aldehydes, except when phosphines with bulky substituents were used, forming predominantly linear products. Notable divergent reactivity between the di- and triphosphine analogues occurred at low loadings and low pressures where the triphosphines maintain branched selectivity, while diphosphines did not.

Kinetic studies demonstrated that increasing H₂ pressure results in a slight rate increase while regioselectivity was negligible. On the other hand, increasing CO pressure dramatically reduces the overall reactivity, and results in some selectivity enhancement towards the branched product. A deuterioformylation study confirmed olefin insertion to be irreversible for the branched pathway and likely regio-determining. The rare selectivity observed in this system likely stems from a trapping of the branched Rh–alkyl species which inevitably forms branched aldehydes, while the corresponding linear Rh–alkyl species shows some reversibility. Mechanistic studies allowed the characterization of several rhodium species that likely exist in a dynamic equilibrium as the catalytic resting state.

AUTHOR INFORMATION

Corresponding Author

*E-mail: nozaki@chembio.t.u-tokyo.ac.jp

Author Contributions

The manuscript was written through contributions of all authors. All authors have given approval to the final version of the manuscript.

Funding Sources

Funds from the Japan Society for the Promotion of Science (JSPS) were used to support the research in this manuscript.

Notes

The authors declare no competing financial interest.

ASSOCIATED CONTENT

Supporting Information.

The following file is available free of charge on the ACS Publications website at DOI: xxx.

Further experimental details; NMR, IR, and mass data; preliminary kinetic analysis; deuterioformylation study results; additional *in situ* high-pressure NMR spectra including variable temperature data; representative GC chromatograms and NMR spectra of aldehyde product identification (PDF)

ACKNOWLEDGMENT

AP is grateful to the JSPS for provision of a JSPS Standard Fellowship (P16338). We are grateful to Jingyuan Deng for proofreading and advice on final manuscript.

REFERENCES

- (1) (a) Cornils, B.; Herrmann, W. A.; Beller, M.; Paciello, R. In *Applied Homogeneous Catalysis with Organometallic Compounds*, 3rd ed.; Wiley-VCH Verlag GmbH & Co. KGaA: Weinheim, Germany, 2018; Vol. 1, p 25–89. (b) Franke, R.; Selent, D.; Börner, A. Applied Hydroformylation. *Chem. Rev.* 2012, 112, 5675–5732.

- (2) (a) van Leeuwen, P. W. N. M. V.; Claver, C. In *Rhodium Catalyzed Hydroformylation*, 1st ed.; Kluwer Academic Publisher: New York, USA, 2002; Vol. 22, p 1–33. (b) Börner, A.; Franke, R. In *Hydroformylation. Fundamentals, Processes, and Applications in Organic Synthesis*, 1st ed.; Wiley-VCH Verlag GmbH & Co. KGaA: Weinheim, Germany, 2016; Vol. 1, p 24–35. (c) Tudor, R.; Ashley, M. Enhancement of Industrial Hydroformylation Processes by the Adoption of Rhodium-Based Catalyst: Part I. *Platinum Metals Rev.* 2007, 51, 116–126. (d) Mahatthananchai, J.; Dumas, A. M.; Bode, J. W. Catalytic Selective Synthesis. *Angew. Chem., Int. Ed.* 2012, 51, 10954–10990.
- (3) (a) Casey, C. P.; Whiteker, G. T.; Melville, M. G.; Petrovich, L. M.; Gavney, Jr., J. A.; Powell, D. R. Diphosphines with Natural Bite Angles near 120° Increase Selectivity for *n*-Aldehyde Formation in Rhodium-Catalyzed Hydroformylation. *J. Am. Chem. Soc.* 1992, 114, 5535–5543. (b) Kranenburg, M.; van der Burgt, Y. E. M.; Kamer, P. C. J.; van Leeuwen, P. W. N. M. New Diphosphine Ligands Based on Heterocyclic Aromatics Inducing Very High Regioselectivity in Rhodium-Catalyzed Hydroformylation: Effect of the Bite Angle. *Organometallics* 1995, 14, 3081–3089. (c) Kalck, P.; Park, D. C.; Serein, F.; Thorez, A. Influence of Various Parameters on the Selectivity of the Production of Aldehydes Starting from Alkenes Issued from the Biomass and Using the Catalyst Precursors $\text{Rh}_2(\mu\text{-SR})_2(\text{CO})_2(\text{PA}_3)_2$. *J. Mol. Catal.* 1986, 36, 349–357. (d) Jiao, Y.; Torne, M. S.; Gracia, J.; Neimantsverdriet, J. W.; van Leeuwen, P. W. N. M. Ligand Effects in Rhodium-Catalyzed Hydroformylation with Bisphosphines: Steric or Electronic? *Catal. Sci. Technol.* 2017, 7, 1404–1414.
- (4) (a) Gual, A.; Godard, C.; Castellón, S.; Claver, C. Highlights of the Rh-Catalysed Asymmetric Hydroformylation of Alkenes Using Phosphorus Donor Ligands.

- Tetrahedron: Asymmetry* 2010, 21, 1135–1146. (b) Agbossou, F.; Carpentier, J.-F.; Mortreux, A. Asymmetric Hydroformylation. *Chem. Rev.* 1995, 95, 2485–2506.
- (5) (a) Nozaki, K.; Sakai, N.; Nanno, T.; Hashiguchi, T.; Mano, S.; Horiuchi, T.; Takaya, H. Highly Enantioselective Hydroformylation of Olefins Catalyzed by Rhodium(I) Complexes of New Chiral Phosphine–Phosphite Ligands. *J. Am. Chem. Soc.* 1997, 119, 4413–4423. (b) Yu, S.; Chie, Y.-M.; Zhang, X. Highly Regioselective and Rapid Hydroformylation of Alkyl Acrylates Catalyzed by a Rhodium Complex with a Tetraphosphorus Ligand. *Adv. Synth. Catal.* 2009, 351, 537–540. (c) Wassenaar, J.; de Bruin, B.; Reek, J. N. H. Rhodium-Catalyzed Asymmetric Hydroformylation with Taddol-Based IndolPhos Ligands. *Organometallics* 2010, 29, 2767–2776. (d) Noonan, G. M.; Copley, C. J.; Mahoney, T.; Clarke, M. L. Rhodium/Phospholane–Phosphite Catalysts Give Unusually High Regioselectivity in the Enantioselective Hydroformylation of Vinyl Arenes. *Chem. Commun.* 2014, 50, 1475–1477.
- (6) Li, H.; Dong, K.; Jiao, H.; Neumann, H.; Jackstell, F.; Beller, M. The Scope and Mechanism of Palladium-Catalysed Markovnikov Alkoxy carbonylation of Alkenes. *Nature Chem.* 2016, 8, 1159–1166.
- (7) (a) da Silva, A. C.; de Oliveira, K. C. B.; Gusevskaya, E. V.; dos Santos, E. N. Rhodium-Catalyzed Hydroformylation of Allylbenzenes and Propenylbenzenes: Effect of Phosphine and Diphosphine Ligands on Chemo- and Regioselectivity. *J. Mol. Catal. A: Chem.* 2002, 179, 133–141. (b) Baber, R. A.; Clarke, M. L.; Heslop, K. M.; Marr, A. C.; Orpen, A. G.; Pringle, P. G.; Ward, A.; Zambrano-Williams, D. E. Phenylphosphatrioxa-Adamantanes: Bulky, Robust, Electron-poor Ligands That Give Very Efficient

- Rhodium(I) Hydroformylation Catalysts. *Dalton Trans.* 2005, 1079–1085. (c) McDonald, R. I.; Wong, G. W.; Neupane, R. P.; Stahl, S. S.; Landis, C. R. Enantioselective Hydroformylation of *N*-Vinyl Carboxamides, Allyl Carbamates, and Allyl Ethers Using Chiral Diazaphospholane Ligands. *J. Am. Chem. Soc.* 2010, 132, 14027–14029. (d) Zuidema, E.; Goudriaan, P. E.; Swennenhuis, B. H. G.; Kamer, P. C. J.; van Leeuwen, P. W. N. M.; Lutz, M.; Spek, A. L. Phenoxaphosphine-Based Diphosphine Ligands. Synthesis and Application in the Hydroformylation Reaction. *Organometallics* 2010, 29, 1210–1221. (e) Dabbawala, A. A.; Jasra, R. V.; Bajaj, H. C. Selective Hydroformylation of 1-Hexene to Branched Aldehydes Using Rhodium Complex of Modified Bulky Phosphine and Phosphite ligands. *Cat. Comm.* 2011, 12, 403–407. (f) Yu, Z.; Eno, M. S.; Annis, A. H.; Morken, J. P. Enantioselective Hydroformylation of 1-Alkenes with Commercial Ph-BPE Ligand. *Org. Lett.* 2015, 17, 3264–3267. (g) How, R. C.; Hembre, R.; Ponasik, J. A.; Tolleson, G. S.; Clarke, M. L. A Modular Family of Phosphine-Phosphoramidite Ligands and Their Hydroformylation Catalysts: Steric Tuning Impacts Upon the Coordination Geometry of Trigonal Bipyramidal Complexes of Type $[\text{Rh}(\text{H})(\text{CO})_2(\text{P}^*\text{P}^*)]$. *Catal. Sci. Technol.* 2016, 6, 118–124.
- (8) (a) Slagt, V. F.; Reek, J. N. H.; Kamer, P. C. J.; van Leeuwen, P. W. N. M. Assembly of Encapsulated Transition Metal Catalysts. *Angew. Chem., Int. Ed.* 2001, 40, 4271–4274. (b) Slagt, V. F.; Kamer, P. C. J.; van Leeuwen, P. W. N. M.; Reek, J. N. H. Encapsulation of Transition Metal Catalysts by Ligand-Template Directed Assembly. *J. Am. Chem. Soc.* 2004, 126, 1526–1536. (c) Kleij, A. W.; Lutz, M.; Spek, A. L.; van Leeuwen, P. W. N. M.; Reek, J. N. H. Encapsulated Transition Metal Catalysts Comprising Peripheral Zn(II)salen Building Blocks: Template-Controlled Reactivity and Selectivity in

- Hydroformylation Catalysis. *Chem. Commun.* 2005, 3661–3663. (d) Kleij, A. W.; Kuil, M.; Tooke, D. M.; Spek, A. L.; Reek, J. N. H. Template-Assisted Ligand Encapsulation; the Impact of an Unusual Coordination Geometry on a Supramolecular Pyridylphosphine–Zn(II)porphyrin Assembly. *Inorg. Chem.* 2005, 44, 7696–7698. (e) Kleij, A. W.; Reek, J. N. H. Ligand-Template Directed Assembly: An Efficient Approach for the Supramolecular Encapsulation of Transition-Metal Catalysts. *Chem. Eur. J.* 2006, 12, 4218–4227. (f) Kuil, M.; Soltner, T.; van Leeuwen, P. W. N. M.; Reek, J. N. H. High-Precision Catalysts: Regioselective Hydroformylation of Internal Alkenes by Encapsulated Rhodium Complexes. *J. Am. Chem. Soc.* 2006, 128, 11344–11345. (g) Bellini, R.; Chikkali, S. H.; Berthon-Gelloz, G.; Reek, J. N. H. Supramolecular Control of Ligand Coordination and Implications in Hydroformylation Reactions. *Angew. Chem., Int. Ed.* 2011, 50, 7342–7345. (h) Bocokić, V.; Kalkan, A.; Lutz, M.; Spek, A. L.; Gryko, D. T.; Reek, J. N. H. Capsule-Controlled Selectivity of a Rhodium Hydroformylation Catalyst. *Nature Comm.* 2013, 4, 1–9. (i) Wang, X.; Nurtila, S. S.; Dzik, W. I.; Becker, R.; Rodgers, J.; Reek, J. N. H. Tuning the Porphyrin Building Block in Self-Assembled Cages for Branched-Selective Hydroformylation of Propene. *Chem. Eur. J.* 2017, 23, 14769–14777.
- (9) (a) Noonan, G. M.; Fuentes, J. A.; Cogley, C. J.; Clarke, M. L. An Asymmetric Hydroformylation Catalyst that Delivers Branched Aldehydes from Alkyl Alkenes. *Angew. Chem., Int. Ed.* 2012, 51, 2477–2480 (b) Pittaway, R.; Fuentes, J. A.; Clarke, M. L. Diastereoselective and Branched-Aldehyde-Selective Tandem Hydroformylation–Hemiaminal Formation: Synthesis of Functionalized Piperidines and Amino Alcohols. *Org. Lett.* 2017, 19, 2845–2848.

- (10) Dingwall, P.; Fuentes, J. A.; Crawford, L.; Slawin, A. M. Z.; Bühl, M.; Clarke, M. L. Understanding a Hydroformylation Catalyst that Produces Branched Aldehydes from Alkyl Alkenes. *J. Am. Chem. Soc.* 2017, 139, 15921–15932.
- (11) Costa, G. N.; Carrilho, R. M. B.; Dias, L. D.; Viana, J. C.; Aquino, G. L. B.; Pineiro, M.; Pereira, M. M. Highly efficient Rh(I)/tris-binaphthyl monophosphite catalysts for hydroformylation of sterically hindered alkyl olefins. *J. Mol. Catal. A: Chem.* 2016, 416, 73–80.
- (12) (a) Busacca, C. A.; Lorenz, J. C.; Grinberg, N.; Haddad, N.; Hrapchak, M.; Latli, B.; Lee, H.; Sabila, P.; Saha, A.; Sarvestani, M.; Shen, S.; Varsolona, R.; Wei, X.; Senanayake, C. H. A Superior Method for the Reduction of Secondary Phosphine Oxides. *Org. Lett.* 2005, 7, 4277–4280. (b) Märkl, G.; Jin, G. Y. N.N.N-Tris(phosphinomethylen)amine, N.N.N'-Tris(phosphinomethylene)hydrazine, N.N'.N'-Tetra(phosphinomethylen)hydrazine. *Tetrahedron Lett.* 1981, 22, 1105–1108. (c) Phanopoulos, A.; White, A. J. P.; Long, N. J.; Miller, P. W. Insight Into the Stereoelectronic Parameters of N-Triphos Ligands *via* Coordination to Tungsten(0). *Dalton Trans.* 2016, 45, 5536–5548.
- (13) (a) Bianchini, C.; Meli, A.; Peruzzini, M.; Vizza, F.; Fujiwara, Y.; Jintoku, T.; Taniguchi, H. Rhodium Complexes with the Tripodal Triphosphine $\text{MeC}(\text{CH}_2\text{PPh}_2)_3$ as Highly Reactive Systems for Hydrogenation and Hydroformylation of Alkenes. *J. Chem. Soc., Chem. Commun.* 1988, 299–301. (b) Bianchini, C.; Meli, A.; Peruzzini, M.; Vizza, F. Tripodal Polyphosphine Ligands in Homogeneous Catalysis. 1. Hydrogenation and

- Hydroformylation of Alkynes and Alkenes Assisted by Organorhodium Complexes with $\text{MeC}(\text{CH}_2\text{PPh}_2)_3$. *Organometallics* 1990, 9, 226–240.
- (14) Rosales, M.; Chacón, G.; González, A.; Pacheco, I.; Baricelli, P. J.; Melean, L. G. Kinetics and Mechanisms of Homogeneous Catalytic Reactions Part 9. Hydroformylation of 1-Hexene Catalyzed by a Rhodium System Containing a Tridentated Phosphine. *J. Mol. Catal. A: Chem.* 2008, 287, 110–114.
- (15) Brezny, A. C.; Landis, C. R. Unexpected CO Dependencies, Catalyst Speciation, and Single Turnover Hydrogenolysis Studies of Hydroformylation via High Pressure NMR Spectroscopy. *J. Am. Chem. Soc.* 2017, 139, 2778–2785.
- (16) (a) Unruh, J. D.; Christenson, J. R. A Study of the Mechanism of Rhodium/Phosphine-Catalyzed Hydroformylation: Use of 1,1'-Bis(diarylphosphino)ferrocene Ligands. *J. Mol. Catal.* 1982, 14, 19–34. (b) Moser, W. R.; Papile, C. J.; Brannon, D. A.; Duwell, R. A.; Weininger, S. J. The Mechanism of Phosphine-Modified Rhodium-Catalyzed Hydroformylation Studied by CIR-FTIR. *J. Mol. Catal.* 1987, 41, 271–292.
- (17) Van der Veen, L. A.; Boele, M. D. K.; Bregman, F. R.; Kamer, P. C. J.; van Leeuwen, P. W. N. M.; Goubitz, K.; Fraanje, J.; Schenk, H.; Bo, C. Electronic Effect on Rhodium Diphosphine Catalyzed Hydroformylation: The Bite Angle Effect Reconsidered. *J. Am. Chem. Soc.* 1998, 120, 11616–11626.
- (18) Casey, C. P.; Paulsen, E. L.; Beuttenmueller, E. W.; Proft, B. R.; Petrovich, L. M.; Matter, B. A.; Powell, D. R. Electron Withdrawing Substituents on Equatorial and Apical Phosphines Have Opposite Effects on the Regioselectivity of Rhodium Catalyzed Hydroformylation. *J. Am. Chem. Soc.* 1997, 119, 11817–11825.

- (19) Kranenburg, M.; van der Burgt, Y. E. M.; Kamer, P. C. J.; van Leeuwen, P. W. N. M. New Diphosphine Ligands Based on Heterocyclic Aromatics Inducing Very High Regioselectivity in Rhodium-Catalyzed Hydroformylation: Effect of the Bite Angle. *Organometallics* 1995, 14, 3081–3089.
- (20) Freixa, Z.; van Leeuwen, P. W. N. M. Bite Angle Effects in Diphosphine Metal Catalysts: Steric or Electronic? *Dalton Trans.* 2003, 1890–1901.
- (21) Wiedner, E. S.; Chambers, M. B.; Pitman, C. L.; Bullock, R. M.; Miller, A. J. M.; Appel, A. M. Thermodynamic Hydricity of Transition Metal Hydrides. *Chem. Rev.* 2016, 116, 8655–8692.
- (22) Axet, M. R.; Castillon, S.; Claver, C. Rhodium-Diphosphite Catalyzed Hydroformylation of Allylbenzene and Propylbenzene Derivatives. *Inorg. Chim. Acta* 2006, 359, 2973–2979.
- (23) Wu, W.; Li, C.-J. A Highly Regio- and Stereoselective Transition Metal-Catalyzed Hydrosilylation of Terminal Alkynes Under Ambient Conditions of Air, Water, and Room Temperature. *Chem. Commun.* 2003, 1668–1669.
- (24) Grünanger, C. U.; Breit, B. Branched-Regioselective Hydroformylation with Catalytic Amounts of a Reversibly Bound Directing Group. *Angew. Chem., Int. Ed.* 2008, 47, 7346–7349.
- (25) (a) del Río, I.; Pàmies, O.; van Leeuwen, P. W. N. M.; Claver, C. Mechanistic Study of the Hydroformylation of Styrene Catalyzed by the Rhodium/BDPP System. *J. Organomet. Chem.* 2000, 608, 115–121. (b) Rosales, M.; González, A.; Guerrero, Y.;

- Pacheco, I.; Sánchez-Delgado, R. A. Kinetics and Mechanisms of Homogeneous Catalytic Reactions Part 6. Hydroformylation of 1-Hexene by Use of Rh(acac)(CO)₂/dppe [dppe = 1,2-bis(diphenylphosphino)ethane] as the Precatalyst. *J. Mol. Catal. A: Chem.* 2007, 270, 241–249.
- (26) Casey, C. P.; Petrovich, L. M. (Chelating diphosphine)rhodium-Catalyzed Deuterioformylation of 1-Hexene: Control of Regiochemistry by the Kinetic Ratio of Alkylrhodium Species Formed by Hydride Addition to Complexed Alkene. *J. Am. Chem. Soc.* 1995, 117, 6007–6014.
- (27) Meakin, P.; Muetterties, E. L.; Jesson, J. P. Intramolecular Rearrangement Mechanisms in Five-Coordinate Complexes. *J. Am. Chem. Soc.* 1972, 94, 5271–5285.
- (28) van der Slot, S. C.; Kamer, P. C. J.; van Leeuwen, P. W. N. M.; Iggo, J. A.; Heaton, B. T. Mechanistic Studies of the Hydroformylation of 1-Alkenes Using a Monodentate Phosphorus Diamide Ligand. *Organometallics* 2001, 20, 430–441.
- (29) Reetz, M. T.; Waldvogel, S. R.; Goddard, R. Substituent Effects in the Rhodium-catalyzed Hydroformylation of Olefins Using Bis(diarylphosphino)methylamino Ligands. *Tetrahedron Lett.* 1997, 38, 5967–5970.
- (30) Bays, J. T.; Priyadarshani, N.; Jeletic, M. S.; Hulley, E. B.; Miller, D. L.; Linehan, J. C.; Shaw, W. J. The Influence of the Second and Outer Coordination Spheres on Rh(diphosphine)₂ CO₂ Hydrogenation Catalysts. *ACS Catal.* 2014, 4, 3663–3670.

- (31) Ternel, J.; Dubois, J.-L.; Couturier, J.-L.; Monflier, E.; Carpentier, J.-F. Rhodium-Catalyzed Homogeneous and Aqueous Biphasic Hydroformylation of the Acrolein Acetal 2-Vinyl-5-Methyl-1,3-Dioxane. *Chem. Cat. Chem.* 2013, 5, 1562–1569.
- (32) (a) Fujita, E.; Muckerman, J. T.; Himeda, Y. Interconversion of CO₂ and Formic Acid by Bio-Inspired Ir Complexes with Pendent Bases. *Biochim. Biophys. Acta* 2013, 1827, 1031–1038. (b) Wang, W.-H.; Hull, J. F.; Muckerman, J. T.; Fujita, E.; Himeda, Y. Second-Coordination-Sphere and Electronic Effects Enhance Iridium(III)-Catalyzed Homogeneous Hydrogenation of Carbon Dioxide in Water Near Ambient Temperature and Pressure. *Energy Environ. Sci.* 2012, 5, 7923–7926.

TOC IMAGE:

